Resistance to Sliding on Atomic Scales in the Adhesive Contact of two Elastic Spheres

C. Dominik and A.G.G.M. Tielens
NASA Ames Research Center
Mail-Stop 245-3
Moffett Field, CA 94035

January 6, 2004

0 Abstract

The structure and stability of agglomerates of micron-sized particles is determined by the mechanical properties of the individual contacts between the constituent particles. In this paper we study the possibility of aggregate rearrangements by sliding. Since the contacts between (sub)micron particles are only a few hundred atoms in diameter, processes on atomic levels will play the dominating roll. We study a theoretical model of sliding friction for surfaces that are either flat or contain steps in their grids. The results show that sliding over flat surfaces may produce a large range of friction coefficients, including zero if the adhesive forces are small compared to the binding forces inside a body. However, both grid alignment and steps in the surface will lead to high values for friction. These processes combined virtually eliminate the possibility of sliding in a collision of two (sub)micron sized particles at velocities low enough for sticking to occur. On the other hand we show that in collisions between aggregates sliding may be an important factor for energy dissipation and compaction.

1 Introduction

Aggregates of micron-sized spherical particles are a subject of increasing importance in a variety of fields. Examples are sooting flames (Kinoshita 1988) and atmospheric pollution.

We are particularly interested in the formation of planetary bodies in the early solar nebula surrounding the protosun. The basic step towards the formation of solid bodies in this environment is the agglomeration of submicron grains into larger aggregates. Interplanetary dust particles which still carry the signature of this collisional assemblage process are now continuously collected in the stratosphere and analyzed in detail in the laboratory (e.g. Brownlee, Pilachowski, Olszewski and Hodge 1979). Understanding the formation and survival of these aggregates is of genuine importance in understanding the origin and evolution of the solar system and planetary systems in general.

Studies of aggregates have in the past often concentrated on mathematical properties like fractal dimensions. Also, physical properties like conductivity have been studied. However, the formation and stability of aggregates depends to a large extend on mechanical properties of the contacts which have so far not attracted as much interest. Kantor and Witten (1984) have looked at the stability of tenuous structures under the assumption of a given strength of the adhesive joint between two particles. However, important for studies like this is the knowledge of the strength of the contact itself, and this is not very well known so far.

A contact between two spheres has a total of six different degrees of freedom, as shown in Fig. 1. In all these degrees, the contact may be subjected to forces (e.g. during a collision of an aggregate with other particles, due to gravitational forces or due to thermal vibrations).

Depending on the direction of the applied forces, the particles may slide, roll or twist over each other, or the contact may break. For a reliable theoretical study of the mechanical properties of such structures, it is therefore vital to understand these processes in detail.

The response of a contact to forces acting in the vertical direction has been studied in most detail. The basis here are the theories of Johnson, Kendall and Roberts (1971) and Derjaguin, Muller and Toporov (1975) which describe the properties of an adhesive contact between elastic spheres under the influence of an applied vertical force. These theories have been used to analyze agglomeration in head-on collisions by Chokshi, Tielens and Hollenbach (1993). The results show that, for low velocities, dissipation by elastic wave excitation during a collision promotes sticking. At high velocities colliding grains will bounce.

The effects of an applied torque that might lead to rolling of the two spheres over each other has recently been studied by Dominik and Tielens (1995, henceforth paper I). It was shown, that a critical force is required to initiate rolling in a contact between two elastic spheres. It was also shown, that aggregates made of very small grains should break rather than allow rearrangement. In contrast, aggregates made of bigger particles allow restructuring by rolling without actually breaking contacts.

In the current paper, we want to discuss the degrees of freedom which involve tangential forces, and torques about the z-axis. When these forces are sufficiently high, they will lead

to sliding or a relative spinning motion of the two spheres in contact. We discuss these two degrees together, since both processes involve the motion of one surface relative to the other in a direction within the contact plane. The resistance to both types of applied force is due to sliding friction.

The response of a contact to tangential forces can in general be calculated from the theory of elasticity when the frictional behavior of the interface is known (e.g. Johnson 1989). From an engineering point of view, the term "friction" stands for a large variety of different physical processes which are involved in dissipating energy when two surfaces slide over each other (Tabor 1992). These processes range from hydrodynamic friction in lubricants, to wear-less energy losses on atomic levels, to plastic deformation of the surfaces during sliding, and to material wear. For an overview, see Tabor (1992). The usual form of the friction law has been motivated by experimental studies which show that in many cases the friction force during sliding, Q_x^{slide} is proportional to the vertical load P, thus

$$Q_x^{\text{slide}} = \mu P \quad . \tag{1}$$

μ is called the coefficient of friction. Later this was reformulated by Coulomb to include the effect of adhesion to

$$Q_x^{\text{slide}} = \mu P + \mu_0 \tag{2}$$

where μ_0 indicates the friction at zero load. This law was first formulated for the friction of a body as a whole. Later, especially in the theory of elasticity, the validity of this law for small surfaces elements was assumed to provide theoretical understanding of sliding processes. The theoretical justification of this law usually invokes the rough structure of the surface, which allows contact only at a few small sites.

However, since this paper deals with micron sized spheres, we are reluctant to simply adapt macroscopic laws for the calculations of friction between colloidal particles. One important feature here is that the contact area between such grains is usually only a few hundred atoms in diameter. Therefore, surface asperities are expected to play only a limited role. Instead, we expect that processes on the level of atomic dimensions dominate friction (Tománek 1993).

Since we are considering the friction between micron-sized spheres which are held together by adhesive forces only, the relevant friction processes are much restricted. The adhesive forces between spheres are often much smaller than the binding forces in the solid materials themselves. Since adhesion is the only force pressing the spheres together, the pressure is usually not sufficient to provide for plastic deformation and wear. Also, hydrodynamic friction will not play a roll at these sizes, since a few atomic layers of a lubricant between the spheres would break the contact between them. The main mechanism that should produce friction in our case are wear-less energy losses on atomic levels (c.f. Tománek 1993, McClelland 1989).

The subject of sliding friction on small scales has drawn considerable interest recently. The development of the scanning force microscope has made direct measurement of microscopic friction possible and has stimulated molecular dynamic simulations of the interaction

of small tips with a surface (Landman, Luedtke, Burnham and Colton 1990, Landman and Luedtke 1993) which show the effects of contact forces in great detail.

The idea that friction is due to dissipative processes on atomic level goes back to Tomlinson. In a beautiful paper (Tomlinson 1929), he discussed friction as a dissipative process on atomic scales, even though by that time not much was known about the interaction between atoms. For his discussion, he described individual atoms as independent oscillators. He also discussed first the importance of adiabadicity and stability of the motion of the atoms for the question of friction. Another early model of friction based on the theory of atomic interactions is due to Derjaguin (1934). An important later development was the Frenkel-Kontorowa model (Frenkel and Kontorowa 1938) which also considered the effects of displacement of the nearest neighbors of the sliding atom. These models have recently been re-discussed by McClelland (1989). He finds that both models show the possibility of a zero friction force for certain model parameters. This intriguing possibility might have important consequences for material sciences. McClelland points out that his models have a qualitative character and the main result taken from the models is that the possibility of zero friction exists.

Tománek (1993) went a step further and attempted to calculate the friction between a tip and a flat surface from first principles. This was possible since he chose a special material combination in which adhesive forces are unimportant. He found reasonable agreement between his calculations and the experiments. However, this approach requires a very detailed knowledge of the properties of the inter-atomic forces. This is up to now only possible in special cases or with extreme computational efforts.

In this paper we want to take a step back and calculate the friction between materials in a very general way. Although undoubtly this general approach will prohibit exact results for friction in a given system, it will give an estimate of the material dependences of friction in such systems and the forces to be expected. The model basically consists of a simple potential for the interaction of two atoms - we follow Tománek's guidance in this.

Another idea that goes back to Tomlinson's early paper is to express the friction properties in terms of the elastic properties of the materials involved. We want to follow this idea in so far as we will express the potential used for the interaction in terms of the elastic properties of the material. Again, this will prohibit exact quantitative results for the friction, but will provide us with a general trend. Furthermore, since the properties of a contact between small particles are well described in terms of the elastic modulus E and surface energy γ, we will have a limited set of parameters to explore in our model.

In Section 2, the energy lost by atoms sliding over a surface will be discussed in the context of the independent oscillator model. We will show, that sliding friction in this picture can be quite high or exactly zero, depending on the parameters of the systems under consideration. In our discussion we will closely follow the studies of McClelland (1989) and Tománek (1993). We will then link the properties of the potential to bulk material properties and derive friction coefficients. In section 3 we will discuss the influence of surface roughness and/or steps in the surface grid and derive a friction coefficient for this case. Section 4 will apply these results to adhesive contacts between elastic spheres and discuss the validity and limitations of this approach. We will summarize our conclusions

in Section 5.

2 Energy losses of a single sliding atom

The most simple approach to study friction on atomic scales in the contact area of two bodies is modeling the individual atoms as independent oscillators. The assumption of independence implies that the total force transmitted in the contact area can be calculated by summing up the contributions of the individual atoms.

In our discussion we will be following many aspects of the contributions by Tománek (1993) and McClelland (1989). We therefore concentrate on the main points and refer the reader to the original works for further details.

The geometry of our model is shown in Fig. 2. The model consists of a substrate A (which for the time being is rigid) and a slider B. The substrate is given by a sequence of atoms with an equal spacing b. The sliding atom is in contact with the substrate and we denote the equilibrium distance between the sliding atom and any substrate atom by σ. The sliding atom now feels forces due to the interaction with the substrate (usually van der Waals interaction) and due to its bonds with the sliding body. We model the tangential part of the binding forces inside the sliding body with a spring characterized by a spring constant c_h. The vertical part of these interactions can be modeled either by a spring (assuming that the second layer of atoms moves at a constant height, not influenced of the contact below) or simply by the assumption of a constant force. Our numerical simulations of both cases show very similar friction results. We use the simpler assumption of a constant vertical force f_z that presses the atom against the substrate.

During sliding, the sliding atom moves in the potential provided by the atoms in the other body. In order to move over the surface, the sliding atom must first overcome the wells in that potential. It must first be pushed out of the potential minimum it is occupying. A certain force is necessary for this, and we will call this force the force necessary to *initiate* sliding. However, once the atom has reached a maximum in the potential, it can move into the next minimum. During this phase it feels a force *in* the direction of its motion and may regain some of the energy spent to overcome the potential well. Thus we are faced with two typical forces:

1. The initial force needed to pull an atom out of a potential minimum on a surface. This force is the maximum force encountered by the sliding atom. It is always different from zero. We will denote it by $f_x^{\max}$.

2. The *average* force needed to keep an atom sliding over a surface. This force might be much lower that $f_x^{\max}$ and it can even be zero. We will call this force f_x^{fric}.

2.1 Model for the potential

Like McClelland, we discuss a two-dimensional case, where sliding proceeds in x-direction, above an axis of symmetry of the A surface - so that the potential is symmetric in y-

direction. Thus we slide over the top of a row of atoms. The atom B moves in a potential

$$V(x,z) = V_{AB}(x,z) + V_{BB}(x,z) \tag{3}$$

which is composed of two different parts. V_{AB} accounts for the interaction between the B atom and the A surface it is sliding upon which we will below. V_{BB} describes the interaction of the B atom with is own neighbors. x, z are the coordinates of the sliding atom B.

The potential V_{BB} is given in terms of the vertical load f_z and the spring constant c_h (c.f. Tománek 1993):

$$V_{BB}(x, x_0, z) = z f_z + \frac{1}{2} c_h (x - x_0)^2 \quad . \tag{4}$$

The potential also depends on a parameter x_0 which accounts for the motion in x-direction of the solid B. x_0 is the equilibrium position of the atom B in the solid - that is the place where it would be without the interaction with solid A:

$$\frac{\partial}{\partial x} V_{BB}(x_0, z) = 0 \quad . \tag{5}$$

In order to specify the potential V_{AB}, we describe the interaction between the sliding atom and the substrate by a superposition of Lennard-Jones Potentials. The pair potential is given by

$$V_{\text{pair}}(r) = 4\varepsilon \left\{ \left(\frac{\sigma}{r}\right)^{12} - \left(\frac{\sigma}{r}\right)^{6} \right\} \tag{6}$$

where r is the distance between the two atoms and $-\varepsilon$ is the minimum energy which corresponds to a distance of $\sigma_{\text{eq}} = \sqrt[6]{2}\sigma$.

Since the substrate is composed of a number of atoms, the total potential is given by a sum over the individual pair potentials.

$$V_{\text{AB}}(x,z) = \sum_i V_{\text{pair}}(r_i) \tag{7}$$

$$r_i = \sqrt{(x - x_i)^2 + (z - z_i)^2} \tag{8}$$

where x_i, z_i are the coordinates of atom i in body A.

We have applied the equations given above to a model of the interface between the two bodies. In this model, the rigid substrate is composed of individual atoms which are positioned in a cubic grid. The surface atoms are placed in the x-y plane. Thus, if one surface atom is located at the coordinates (0,0,0), its nearest neighbors are (b,0,0), (-b,0,0), (0,b,0), (0,-b,0), and (0,0,-b), where b is the distance between two neighboring atoms. In the calculations a total of 78 atoms where placed in the range $-6b \le x_i \le 6b$, $-b \le y_i \le b$, $-b \le z_i \le 0$. The calculation was carried through in dimensionless form by normalizing all quantities by the parameters of the Lennard-Jones potential that acts between the substrate atoms and the test atom. Thus we used the following units:

length:	σ
energy:	ε
force:	ε/σ
spring constant:	ε/σ^2

In most calculations we also put $b = \sigma$. During the calculations we calculate the potential $V(x, x_0)$ for x in the range (-b,b).

Figure 3 shows the potential V_{AB} and its derivatives as a function of x, in the case of $f_z = 0$. The substrate atoms are located at $x = -1$, $x = 0$, and $x = +1$. It can be seen that the potential has a slightly corrugated cosine shape. The force in x-direction (f_x) is shown in the dashed line. f_x is point-symmetrical around the position of the substrate atom. The maximum value of f_x is reached at $x \approx \pm 0.37$. The bottom plot shows the negative value of the second derivative of the potential V_0 which can be used to check for the possibility of instabilities (see Eq. (14) and below in the text).

2.2 Instabilities

According to McClelland (1989) and Tománek (1993), energy will be lost by the sliding atom if there occur instabilities in the motion of the atom. These instabilities depend on the ratio of the interactions described by the potentials V_{AB} and V_{BB}, respectively, and is connected with the occurrence of a saddle point in the total potential.

For the discussion of the instabilities in the motion we write the potential as effective function of a single coordinate. We can get z as a function of x from the condition

$$\frac{\partial}{\partial z} V(x, x_0, z) = 0 \tag{9}$$

and rewrite the potential as

$$\begin{aligned} V(x, x_0) &= V_{AB}(x, z(x)) + z(x) f_z + \frac{1}{2} c_h (x - x_0)^2 & (10) \\ &=: V_0(x) + \frac{1}{2} c_h (x - x_0)^2 \quad . & (11) \end{aligned}$$

The sliding of the atom over the surface can now be modeled by a motion of the point x_0 and we can calculate the position $x(x_0)$ of the sliding atom as well as the involved forces. The equilibrium $x(x_0)$ position of the atom is obtained from

$$\frac{\partial}{\partial x} V(x, x_0) = 0 \tag{12}$$

and the force that must be applied to the sliding atom in order to keep it in this position is

$$f_x(x(x_0), x_0) = c_h (x_0 - x) \quad . \tag{13}$$

It is clear that when the solution $x(x_0)$ is unique and smooth everywhere, the motion is reversible and no energy is dissipated. For a detailed discussion of this see McClelland (1989). However, if the solution $x(x_0)$ is not unique, there will be jumps in the motion of the sliding atom, and in these jumps energy will be dissipated. Since a jump occurs when a saddle point in the total potential $V(x, x_0)$ occurs, the condition for no dissipation is

$$c_h > -\frac{\partial^2}{\partial x^2} V_0(x, x_0) \quad . \tag{14}$$

Thus, if the horizontal spring constant c_h is larger than $\max_{x(x_0),x_0} \left(-\frac{\partial^2}{\partial x^2}\right) V(x, x_0)$, the sliding of the atom occurs smoothly and without dissipation.

However, if c_h is smaller than this value, the sliding atom may stay behind a certain substrate atom even though the point x_0 has already moved beyond the position of the substrate atom. Eventually, the sliding atom will move over that atom and jump forward, dissipating some of its energy.

From Fig. (3) we may infer the critical value for the spring constant in the case of no external force applied. The maximum of $-\partial^2 V_{AB}/(\partial x^2)$ is approximately 9. Thus for spring constants $c_h \lesssim 9$ we will have to expect instabilities and thus energy dissipation.

Figure 4 shows the simulation of the sliding motion. In this simulation, x_0 was moved into positive x direction. The equilibrium position of x was then calculated. Since at times, the solution for $x(x_0)$ was not unique, the solution closest to the last one was used. When the simulation met a point, where no stable solution for $x(x_0)$ could be found close to the last equilibrium position, a jump point was diagnosed. The atom was then moved further in positive x direction to the next available stable position. The energy difference between the two positions was considered to be lost.

Figure 4 shows forces and positions as functions of x_0. The three different rows of diagrams correspond to different normal forces f_z. It can be seen that for small normal forces, $x(x_0)$ is unique and no jumps occur. The motion of the sliding atom is smooth, sometimes lagging, sometimes preceding the motion of the equilibrium position (i.e. the rest of the solid). The average force (the friction force) in this case is zero. However, with increasing f_z, the lagging/preceding motion gets more pronounced until the sliding atom gets "trapped" behind a substrate atom. Then, $x(x_0)$ is not unique and jumps occur in the motion of the atom. The friction force starts to differ from zero, an effect that becomes more pronounced as f_z increases.

From our model, we can define the two forces important for friction. The critical force that is needed to move the atom out of its potential minimum on the substrate surface is given by the maximum of f_x:

$$f_x^{\max} = \max_{x(x_0),x_0} \{c_h \left(x_0 - x(x_0)\right)\} \quad . \tag{15}$$

The force needed to keep the atom sliding is the mean force in x-direction during the motion of x_0. If the potential V_{AB} is periodic in x-direction over a length ℓ, it is sufficient to take the mean over this length.

$$f_x^{\rm fric} = \frac{1}{\ell}\int_0^\ell f_x(x(x_0),x_0){\rm d}x_0 \quad . \tag{16}$$

Figure 5 summarizes the results of many simulations like the one described above. We have plotted the dependence of the maximum force, the critical spring constant, and the friction force on the applied normal force f_z. The results show that the force needed to initiate sliding and the average friction force increase with increasing applied force. Likewise, the critical spring constant $c_{\rm crit}$ below which there is not friction increases monotonically with increasing f_z. Essentially, for increasing f_z, a better "coupling" of the atom with the rest of the slider is required in order to avoid friction.

The relationship between f_z and $c_{\rm crit}$ can be inverted. For a fixed horizontal spring constant, this then defines a critical normal force $f_z^{\rm crit}$ which must be applied in order to get friction. Obviously, $f_{z,{\rm crit}}$, $f_x^{\rm max}$ and $f_x^{\rm fric}$ can be fitted to good accuracy in the following way:

$$f_z^{\rm crit} = \alpha_1 c_h + \beta_1 \tag{17}$$

$$f_x^{\rm max} = \alpha_2 f_z + \beta_2 \tag{18}$$

$$f_x^{\rm fric} = \begin{cases} \alpha_3\left(f_z - f_z^{\rm crit}\right) & : \quad f_z > f_z^{\rm crit} \\ 0 & : \quad f_z \le f_z^{\rm crit} \end{cases} \tag{19}$$

where α_1, α_2, α_3, β_1, and β_2 are constants. In our model, these constants are

$$\alpha_1 = +0.89 \tag{20}$$

$$\alpha_2 = +0.34 \tag{21}$$

$$\alpha_3 = +0.33 \tag{22}$$

$$\beta_1 = -8.24 \tag{23}$$

$$\beta_2 = +3.07 \tag{24}$$

2.3 The material properties

In order to apply the results of the dimensionless calculation to a physical system, ε, σ, and c_h have to be specified. We will again resort to a very simple approach which relates the properties of the bulk material to the quantities in our approach. The advantage of this is that the sliding properties are expressed in terms of the same quantities that characterize the adhesive contact itself.

First, we need the energy ε associated with the adhesive force between the two surfaces. In order to choose this value consistently we consider the interaction energy per unit surface area between two surfaces at a distance r as derived from Hamakers treatment (e.g. Israelachvili 1992)

$$W_{\text{surface}}(r) = -\frac{A_H}{12\pi r^2} \tag{25}$$

where $A_H = \pi^2 C n_1 n_2$ is Hamakers constant. C is the interaction constant for the atom-atom interaction which is given in the frame of our model by $C = 4\varepsilon\sigma^6$. We get

$$A_H = 4\varepsilon\pi^2\sigma^6 n_1 n_2 \tag{26}$$

with $n_i \approx b_i^{-3}$ being the number density of atoms in each solid. At a separation σ the energy is the given by

$$W_{\text{surface}}(\sigma) = -\varepsilon\frac{\pi}{3}\frac{\sigma^4}{b^6} \quad . \tag{27}$$

b is here given by $b = \sqrt{b_1 b_2}$. This energy is the surface energy γ. Thus we have

$$\varepsilon = \frac{3}{\pi}\frac{b^6}{\sigma^4}\gamma \tag{28}$$

defining ε in terms of known material properties.

We assume that the horizontal spring constant of a single atom can be derived from the shear modulus of the material. At this point we can relax the assumption of the rigidity of the substrate. Let the atoms in the substrate surface interact with the rest of the substrate with a force given by a spring constant just like the one for the slider. Then one can easily show that the effective spring constant (the ratio of the force and the relative displacement of the two bodies) is the geometric mean of c_h for both bodies. With G the reduced shear modulus of the two materials ($1/G = 1/G_1 + 1/G_2$) and b the typical distance between atoms in the bulk material, we may write the dimensionless spring constant as

$$c_h = \frac{Gb}{\varepsilon/\sigma^2} = \frac{G\sigma^2}{\gamma b} \quad . \tag{29}$$

2.4 Application to real contacts

A major difficulty in applying the results obtained to real contact areas between grains is the assumption of the atom being an independent oscillator. This assumption implies that the forces acting on the atom are independent from the positions of the nearest neighbors of the sliding atom in the slider. Clearly, this is only true if the there are no interactions between the sliding atom and its neighbors, or if those neighbors do not change their position. Both possibilities are generally not valid. The positions of the neighbors do influence the acting forces and the neighbors move due to both their own interaction with the substrate and with their neighbors. However, if these motions are completely uncorrelated with the motion of the sliding atom itself, the average situation will be similar to the independent case. The motion of the neighbor atoms will be uncorrelated only if the two atomic grids that are sliding over each other are not commensurable - i.e. the distance between atoms in the sliding direction in one body must not be an integer multiple of

the same quantity in the other body (McClelland 1989,1992). This can be true for two different materials. It can also be accomplished by two identical grids that are not properly aligned. (see discussion in Reiss (1968)). In these cases the independent oscillator model will be reasonably applicable. Furthermore, the independent oscillator gives a lower limit for the total friction, since the effects of in-phase acting atoms will increase the resistance to sliding. This is further justified by studies of McClelland (1989) of the Frenkel-Kontorowa model. He finds that the transition between friction and zero friction occurs at about the same physical parameters (within a factor of 2) as in the independent oscillator model.

If two grids are commensurable, all the atoms will be in phase and the resulting force will be very large - of the order of the maximum force that can be sustained by all atoms in the contact area. Sliding will then occur in a slip-stick motion. In this type of motion, essentially the whole contact does not slide until a critical force is reached. Then, the surfaces in contact start to slip everywhere at once, and they slide for some distance before they come to rest again. The procedure is repeated. The average force in this case will again be of the order of the maximum force.

It is therefore not possible to use the independent oscillator model to calculate the frictional forces in general. However, it may well be used to derive two limiting cases.

1. The minimum friction force. This is given by the integral of the friction force of the independent oscillator over the contact area.

2. The maximum friction force. This is the maximum force possible for each individual atom, integrated over the contact area.

We evaluate these two limiting cases in order to derive pressure-traction relations that can later be applied to the pressure distribution in the contact.

2.5 Translation of the atomic friction results in a pressure - tangential tractions relation

We can find the tractions due to friction in the contact area from Eq. (18) by multiplicating Eq. (18) by $\varepsilon/(\sigma b^2)$ and substituting ε from Eq. (28). The result is a Coulomb-type bimodal friction formula (c.f. Equation (2)).

$$q^{\max,\mathrm{io}} = \mu^{\max,\mathrm{io}} p + \mu_0^{\max,\mathrm{io}} \quad . \tag{30}$$

The superscript "io" has been added in order to distinguish the tractions in the independent oscillator case from other tractions. The coefficients are given by

$$\mu^{\max,\mathrm{io}} = \alpha_2 \tag{31}$$

$$\mu_0^{\max,\mathrm{io}} = \frac{3\beta_2}{\pi}\frac{b^4}{\sigma^5}\gamma \quad . \tag{32}$$

Similarly, we can transform the equation for the friction during sliding (Eq. (19)). Again we get a Coulomb-type formula

$$q^{\text{slide,io}} = \begin{cases} \mu^{\text{slide,io}} p + \mu_0^{\text{slide,io}} & : \quad p > p_{\text{crit}} \\ 0 & : \quad p \leq p_{\text{crit}} \end{cases} \quad . \tag{33}$$

p_{crit} is the critical pressure that is necessary for the onset of friction

$$p_{\text{crit}} = \frac{3\alpha_1}{\pi} \frac{b^3}{\sigma^3} G + \frac{3\beta_1}{\pi} \frac{b^4}{\sigma^5} \gamma \quad . \tag{34}$$

If the pressure is less than that, no friction can be expected in the independent oscillator approximation from this part of the contact.

The friction coefficients are given by

$$\mu^{\text{slide,io}} = \alpha_3 \tag{35}$$

$$\mu_0^{\text{slide,io}} = -\alpha_3 p_{\text{crit}} \quad . \tag{36}$$

All four constants $\mu^{\text{max,io}}$, $\mu_0^{\text{max,io}}$, $\mu^{\text{slide,io}}$, and $\mu_0^{\text{slide,io}}$ are material properties which are independent of the normal force.

3 Effects of Surface Roughness

The model of the independent oscillator discussed in the previous section was explicitly limited to the case of sliding of atoms over a flat surface - i.e. over a clean cut of a crystal along one of its major crystal planes. However, this paper is aimed at the processes between two spherical particles. A spherical particle cannot have this type of clean cuts everywhere on its surface. There will be limited regions where the surface approximates this structure. However, there must be other regions where steps in the grid structure occur.

To illustrate this point, we show a three dimensional model constructed of small cubes in such a way that it's shape approximates a sphere. The edge length b of the cubes is 1/100 of the diameter of the sphere. We have chosen cubes as the basic elements because the picture is then more easily to view and interpret. Small spheres would be possible as well. The main planes (1/0/0), (0/1/0), (0/0/1) are easily recognized as well as other important planes like (1/1/0), (1/0/1), (0/1/1), and even (1/1/1). Around the (1/0/0), (0/1/0), and (0/0/1) cuts, the surface is indeed smooth and the independent oscillator model is most suited for these locations. However, most of the surface of the sphere is covered by regions which have a step in the surface grid structure every few atoms (building cubes). In these regions, friction cannot be described in the frame used above, since the force acting on a single atom that is about to surmount a step may be very large. In fact, two spheres in adhesive contact will tend to flatten these steps throughout the contact region as the local pressures at the steps will be higher than in between the steps. When the two spheres are sliding over each other, new steps will be entering the contact area, and the atoms forming

the steps will be depressed into the surfaces. If only one of the surfaces contains steps, it is still conceivable, that the step moves smoothly into the increasing pressure in the contact region. However, when both surfaces contains steps, the meeting of two steps will provide a strong resistance to sliding. This is shown in Fig. (7). When the surfaces move on, the tangential pressure will be strong enough to depress the edge atoms into the respective surfaces. It is unlikely that the energy needed to do this can be regained later in the same way as in the case of a flat surface.

To estimate the energy needed to push an atom into a surface, we again use (for reasons of both simplicity and consistency) values derived from the elastic properties of the bulk materials. In order to press one atom in between two others, the other two atoms have to be separated. We approximate the force necessary to do this be a spring constant

$$c \approx Gb \quad . \tag{37}$$

Therefore the energy needed to push one atom in between of two others is of the order

$$U_{\text{step}} \approx \frac{1}{2} G b^3 \quad . \tag{38}$$

This is similar to Frenkel's calculation of the theoretical sheer strength of a crystal (c.f. Kittel 1976). In order to estimate the total energy that is needed during sliding, we have to determine the number of steps that have to be flattened per unit length of sliding distance. To do so, we observe (again from Fig. 6), that the number of steps along any circumference of the sphere is approximately $2R/b$. The number per unit length is therefore $1/(\pi b)$. A unit surface area thus contains on average $\approx 1/(\pi b^2)$ steps in the direction of its motion. Since the same is true for the second surface, the number of matching steps that have to be flattened per surface area and sliding distance is $1/(\pi^2 b^3)$. With the energy loss (Eq. (38)) this translates into a constant friction coefficient

$$\mu_0^{\text{slide,steps}} = \frac{G}{2\pi^2} \quad . \tag{39}$$

This is a friction term that applies over the whole contact area and is therefore analogous to $\mu_0^{\text{max,io}}$ as defined in Eq. (32). The magnitude of this term compared to the friction terms derived from the independent oscillator model will be discussed in the next section.

4 Resistance to sliding and spinning in a JKRS contact

In the following we derive expressions for friction forces due to the different mechanisms discussed in the previous two sections in closed form. To do that we need to specify the pressure distribution in the contact area.

4.1 The pressure distribution in the JKRS solution of the contact problem with adhesion

The pressure distribution inside the contact area of an adhesive contact between elastic bodies has been calculated by Johnson *et al.* (1971) (JKR) and also by Sperling (1964).

Two elastic adhesive spheres make contact over a finite circular region. In the absence of applied external forces, the radius of this contact area is

$$a_0 = \left(\frac{9\pi\gamma R^2}{E^*}\right)^{1/3} \quad , \tag{40}$$

where γ is the surface energy of each surface in the case of equal materials. For different surfaces, $\gamma = \gamma_1 + \gamma_2 - 2\gamma_{12}$, where γ_{12} is the interface energy. R is the reduced radius of the two spheres ($R^{-1} = R_1^{-1} + R_2^{-1}$) and $(E^*)^{-1} = (1-\nu_1^2)/E_1 + (1-\nu_2^2)/E_2$, where E_i and ν_i are Young's modulus and Poisson's ratio, respectively, of grain i.

In order to separate the two bodies in contact, a critical force is necessary. This is the *pull-off force*

$$P_c = 3\pi\gamma R \quad . \tag{41}$$

In the case of non-zero external force the following relation between the applied load P and the contact radius a holds:

$$\frac{P}{P_c} = 4\left(\widehat{a}^3 - \widehat{a}^{3/2}\right) \tag{42}$$

where $\widehat{a} = a/a_0$. The distribution of pressure in the contact area is given by

$$p(r,a) = 6\frac{P_c}{\pi a_0^2}\widehat{a}\left(1 - r^2/a^2\right)^{1/2} - 2\frac{P_c}{\pi a_0^2}\widehat{a}^{-1/2}\left(1 - r^2/a^2\right)^{-1/2} \quad . \tag{43}$$

This pressure distribution can be used to calculate the distribution of tractions in the contact region. Thus we follow the theory of elasticity in this calculation. However, we will not go into a detailed discussion including microslip near the edge of the contact region (e.g. Johnson 1989). In the calculation of friction forces, the tangential tractions will be integrated without consideration of this effect.

At the end of the section the magnitude of the calculated friction forces will be discussed.

4.2 Sliding

Resistance to sliding is a force that opposes the attempt to slide a body on the surface of another body. If a force Q_x is necessary to slide a sphere over a surface, this force must be balanced by an equal and opposite integral over the tangential traction in the contact area:

$$Q_x = \iint q_x \mathrm{d}x\mathrm{d}y \quad . \tag{44}$$

In order to calculate this integral we use the pressure distribution given by the JKRS theory (Eq. (43)) along with the relations between pressure and tangential traction derived in the previous sections. This has to be done for the three different cases: maximum and average force in the independent oscillator model, and surface grid steps.

4.2.1 The maximum force for matching grids in the independent oscillator model

The maximum tangential force that can sustained in a contact area is given by

$$Q_x^{\max} = 2\pi \int_0^a r q^{\max}(r) \mathrm{d}r \quad . \tag{45}$$

$q^{\max}$ is given in Eq. (30). Integration yields

$$Q_x^{\max} = \mu^{\max} P + \pi a^2 \mu_0^{\max} \quad . \tag{46}$$

4.2.2 The average friction force for non-matching grids in the independent oscillator model

The average force during sliding can be obtained in a similar manner. However, since in general the integral has to be taken only over the central part of the contact region where the pressures exceed p_{crit}, the full solution is somewhat more involved.

p_{crit} is the yield pressure for the onset of friction as defined in Eq. (34). We define a radius r_c where the pressure in the contact region equals p_{crit}:

$$p(r_c, a) = p_{\mathrm{crit}} \quad . \tag{47}$$

Integrating the tractions over that part of the contact area where $p \geq p_{\mathrm{crit}}$ yields

$$\begin{aligned} Q_x^{\mathrm{slide,io}} &= 4\mu^{\mathrm{slide,io}} P_c \left\{ \widehat{a}^3 \left(1 - \sqrt{1 - r_c^2/a^2}^{\,3} \right) - \widehat{a}^{3/2} \left(1 - \sqrt{1 - r_c^2/a^2} \right) \right\} \\ &+ \pi r_c^2 \mu_0^{\mathrm{slide,io}} \quad . \end{aligned} \tag{48}$$

For very low values of P, $p < p_{\mathrm{crit}}$ everywhere in the contact region. Thus, in this case, $r_c = 0$ and the average friction force is zero. The opposite limit is reached when P is very large so that almost the whole contact area contributes to the friction, i.e. $r_c \approx a$. Then, Eq. (48) simplifies in analogy to Eq. (46) to

$$\begin{aligned} Q_x^{\mathrm{slide,io}}(r_c = a) &= 2\pi \int_0^a q_x^{\mathrm{slide,io}} \mathrm{d}r & (49) \\ &= \mu^{\mathrm{slide,io}} P + \pi a^2 \mu_0^{\mathrm{slide,io}} \quad . & (50) \end{aligned}$$

4.2.3 The friction force due to grid steps on surfaces

The friction force due to steps in the surfaces of the spheres is given by

$$\begin{aligned} Q_x^{\text{slide,steps}} &= \pi a^2 \mu_0^{\text{slide,steps}} \\ &= \frac{Ga^2}{2\pi} \end{aligned} \tag{51}$$

4.3 Torsion and Spin

If the two spheres rotate about the z axis at different speeds, the contact area is subjected to a twisting motion. If we assume that adhesion is strong enough to prevent any relative motion in the contact area, the torque M_z due to a relative twist over an angle of $\delta_{\alpha z}$ is given by (Johnson 1989)

$$M_z = \frac{16}{3} G a^3 \delta_{\alpha z} \tag{52}$$

where G is the reduced shear moment of the two materials in contact: $1/G = 1/G_1 + 1/G_2$.

We now proceed as in the section about sliding, since in this case the surfaces also have to slide upon each other in order to allow for a relative motion. In the twisting motion, the tangential tractions in the contact area are all circumferential. The maximum traction that can be sustained if all the atoms are acting in phase is dependent upon the normal pressure p and is given by Eq. (30). When the atoms are not in phase, the average friction force from the independent oscillator model (Eq. (33)) and the resistance to sliding form the surface steps Eq. (39) apply.

4.3.1 The maximum torque for aligned identical grids

Since in the circular contact region under twist, the radius vector and the traction are always perpendicular to each other, the maximum moment that can be reached is given by

$$M_z^{\max} = 2\pi \int_0^a r^2 q^{\max}(r) \mathrm{d}r \quad . \tag{53}$$

With p given by Johnson's solution we get

$$M_z^{\max} = \pi \mu^{\max} P_c a_0 \left(\frac{3}{4} \widehat{a}^4 - \widehat{a}^{5/2} \right) + \frac{2}{3} \pi a^3 \mu_0^{\max} \quad . \tag{54}$$

4.3.2 The torque for unaligned grids

The torque that results when the grids are unaligned can be obtained analogous to the above calculations. Again, the integral has to be taken only over the central part of the contact region:

$$M_z^{\text{slide,io}} = 2\pi \int_0^{r_c} r^2 q^{\text{slide,io}} \mathrm{d}r \tag{55}$$

$$= 2\pi \int_0^{r_c} r^2 \left(\mu^{\text{slide,io}} p(r,a) + \mu_0^{\text{slide,io}}\right) \mathrm{d}r \quad . \tag{56}$$

With Johnson's pressure distribution the result is ($\widehat{r}_c = r_c/a_0$)

$$\begin{aligned} M_z^{\text{slide,io}} &= 2\mu^{\text{slide,io}} P_c a_0 \left[\left(\frac{3}{4}\widehat{a}^4 - \widehat{a}^{5/2}\right) \arcsin\frac{r_c}{a} \right. \\ &\quad \left. + \left(\frac{3}{2}\widehat{a}\widehat{r}_c^3 - \frac{3}{4}\widehat{a}^3\widehat{r}_c + \widehat{a}^{3/2}\widehat{r}_c\right)\sqrt{1 - r_c^2/a^2}\right] \\ &+ \frac{2}{3}\pi r_c^3 \mu_0^{\text{slide,io}} \quad . \end{aligned} \tag{57}$$

In the limit $r_c \to a$, Eq. (57) gives in analogy to Eq. (54)

$$M_z^{\text{slide,io}}(r_c = a) = \pi\mu^{\text{slide,io}} P_c a_0 \left(\frac{3}{4}\widehat{a}^4 - \widehat{a}^{5/2}\right) + \frac{2}{3}\pi a^3 \mu_0^{\text{slide,io}} \quad . \tag{58}$$

4.3.3 The torque due to surface steps

The torque that is due to surface steps is given by

$$M_z^{\text{steps}} = 2\pi\mu_0^{\text{slide,steps}} \int_0^a r^2 \mathrm{d}r = \frac{Ga^3}{3\pi} \tag{59}$$

4.4 Discussion of the forces and the different processes

In general, the forces that resist sliding and spinning, respectively, are dependent on the vertical load that is applied to the contact. When the vertical load increases, so do (in general) the friction forces. However, for a discussion of the dependences of the friction processes on material properties, it is convenient to consider the case with zero applied normal load.

One can show that in this case the friction forces in units of the pull-off force are to very good approximation a function of the particle radius R and the ratio $E\sigma/\gamma$. In the independent oscillator model, the critical parameter for friction is the ratio of the vertical force f_z to the horizontal spring constant c_h. Noting that G is related to E by $G = E/(2(1+\nu))$ and neglecting the factor σ/b one can show that both the central pressure in the JKRS theory divided by the pull-off force ($4P_c/(\pi a_0^2 P_c)$, see Eq. (43)) and the horizontal spring constant ($G\sigma^2/(\gamma b)$, see Eq. (29)) are only dependent on this ratio.

Therefore, the friction forces between two spheres can be plotted in a plane formed by the reduced particle radius and the dimensionless quantity given above.

Fig. 8 shows this kind of force plots of the three different cases discussed in the previous sections for the case of zero normal load. Since all the material properties are combined in a single expression, any given material can be assigned to a position on this axis. We have marked the position of several materials on the top of the plot. The material properties used are shown in table 1. In the plots, all forces are normalized to the pull-off force. Although this does not give direct access to the absolute values of the forces, it reflects the fact, that all typical forces within an aggregate should be of the order of the pull-off forces.

The maximum force obtained from the independent oscillator model is larger than the pull-off force for almost all materials and particle radii considered in this plot. The only exception are very small grains with very high $E\sigma/\gamma$ ratios, like 100Å Quartz spheres. Apart from this exception, attempts to start sliding from a state in which this high friction force applies are very likely to break the contact instead of shifting it by sliding. For large spheres made of materials with low $E\sigma/\gamma$ the friction force exceeds the pull-off force.

A completely different behavior can be seen for the average friction force in the independent oscillator model, which applies when the atomic grids on the surface are different, so that each atom can be viewed as moving independent of its neighbors. Here, the friction can still be very high for materials with low $E\sigma/\gamma$. But there exists an almost vertical dividing line at $E\sigma/\gamma \approx 10^{1.4}$. This value can be readily understood. From Fig. (5) we observe that a spring constant $c_h \lesssim 10$ is required in order to get friction in the case of $f_z = 0$. Since $c_h \approx G\sigma/\gamma$ we find that the condition for friction to occure is

$$\frac{E\sigma}{\gamma} = \frac{2(1+\nu)G\sigma}{\gamma} \approx 2.5c_h \lesssim 25 \quad , \tag{60}$$

which is roughly $10^{1.4}$.

Adhesive contacts of materials with smaller values of this ratio have roughly the same friction as the maximum force calculated above. However, adhesive contacts of materials with a higher value don't have any friction as the result from the independent oscillator model.

Fig. 8c shows the friction that arises from steps in the surface of the spheres. This term is small for very small spheres, mainly because the average number of steps in the contact area is close to zero. However, for spheres larger that 1μm the friction force is of the same order as the pull-off force. For even larger particles, the contribution of this process increases further and may reach 10 to 100 for cm sizes.

The last plot in Fig. 8 shows the sum of the average force from the independent oscillator model and the force due to steps in the surface grid. It is this force that we expect to act on most parts of the surface, unless the two grids are so well aligned that collective effects become important. The figure basically shows, that for materials with $E\sigma/\gamma$ less than the critical value discussed above, sliding inside an aggregate appears to be virtually impossible without threatening the integrity of the aggregate. However, this is not true for materials with supercritical $E\sigma/\gamma$. As long as the individual particles are smaller that about 0.1μm,

the friction force is smaller or of the same order as the pull off force. Thus, in this case, restructuring processes due to sliding are possible.

Figure 9 shows plots similar to Fig. (8), but for the torsional forces. All torques plotted in there are normalized to $P_c a_0$. The results here are qualitatively similar to those given above. This is not surprising, since the basic physical processes for the friction are the same in both processes. The quantitative similarity is due to the use of normalized quantities.

4.5 Sliding in collisions between particles

The magnitude of the friction forces already indicates, that sliding will not be very important in a typical aggregate where all forces cannot be much higher that the pull-off force. To illustrate, we conduct a thought experiment as sketched in Fig. 10. A non-rotating sphere collides tangentially with another sphere that cannot be moved around. The kinetic energy of the moving sphere is W_0. After making contact, the spheres might start sliding over each other. The friction force will be approximately $Q_x^{\mathrm{fric}} := Q_x^{\mathrm{slide,io}} + Q_x^{\mathrm{slide,steps}}$. Thus, in order to dissipate the energy W_0, the sphere may slide a distance

$$s_{\mathrm{slide}} = \frac{W_0}{Q_x^{\mathrm{fric}}} \quad . \tag{61}$$

When we look at a typical collision in which the spheres will stick rather that rebounce, the kinetic energy will be of order $P_c\delta_0$ (Chokshi *et al.* 1993). In Fig. 11 the sliding distance has been plotted in units of the circumference of one sphere. Thus, a value of 1 for the sliding distance means, that the sphere would slide once around the fixed sphere. However, the numbers indicate, that this will never happen. Sliding is only a tiny fraction of $2\pi R$. For materials with $E\sigma/\gamma \gtrsim 10^{2.8}$, no sliding at all happens ($s_{\mathrm{slide}} < b$). This seems to be a contradiction to the results found in Sect. (4.4) were we found that sliding is more easily possible for materials with large $E\sigma/\gamma$. However, fig. (11) also contains information about the maximum velocity at which sticking will be possible. Since this velocity drops rapidly with increasing E and decreasing γ, the collision velocity considered in Fig. (11) is very low for high $E\sigma/\gamma$. Then, the momentum of the colliding spheres is insufficient to provide for the force needed to initiate sliding.

Thus it is quite clear, that in a collision between two identical spheres, sliding will be unimportant. However, in a collision of large aggregates, the kinetic energy of the aggregate is much higher than that of the few contact-making particles. In this case, sliding will be important and can contribute to the compaction of aggregates in collisions.

4.6 The alignment of grid structures

Our results indicate, that both for sliding and spinning the friction forces are considerably increased, when the grids are aligned. In the cases, where sliding and spinning are possible at all (high $E\sigma/\gamma$, flat surface pieces) a possible process is therefore, that the two spheres start in a state where the grids are not aligned and continue to slide or spin until grid alignment takes place. The then much increased friction forces would then stop the relative

motion and freeze in the aligned state. However, the areas on the surface of a sphere that will allow this occupy only a small fraction of the surface (Fig. 6). When these surfaces are sliding over each other, the contact will very probably move out of this region before the grids can be alligned. Therefore, we do not expect that the allignment of grids plays an important role during aggregate formation and/or restructuring.

5 Conclusions

In this paper we have studied the resistance to sliding in an adhesive contact of two elastic spheres. Since we are mainly interested in the physics of aglomerates, our contribution concentrates on the processes between (sub)-micron sized particles.

For particles of this size, the contact area is quite small, only a few hundrets of atoms in diameter. Thus processes on atomic level should play a major role in frictional energy dissipation. We have looked at two different processes that may dissipate energy during the sliding process. First, the motion of atoms over a flat substrate was studied following the work of Tománek (1993) and McClelland (1989,1992). It was shown that sliding friction from this process will be very small when the binding forces inside one body are much greater than the interaction through the interface. It was shown that the critical value for the spring constant characterizing the binding forces inside a body must not exceed a value of ≈ 10 when measured in the units ε and σ of the atom pair potential through the interface. Thus materials like Quarz will expearience no friction from this process as long as the attractive forces in the interface are only van der Waals forces and not chemical bonds. The situation is different for metals or ice, since here the forces through the surface are of the same order as the forces inside a body. This type of materials will infact expearience friction from this first friction process.

We then discussed the effect of steps in the surface grids which will be unevitably present on the surface of roughly spherical particles. A simple estimate showed that these grid steps will provide a strong resistance to sliding for not too small particles. Very small particles are an exception since the contact area is so small that none or only few steps will be present inside the contact at a given time. However, particles larger than about 10^{-7}m will feel friction forces of the order of the pull-off force. In particular this is also the case for materials that are friction free in the flat surface case.

When adding the two contributions together we find that sliding friction is of the order of the pull-off force P_c or greater for allmost all radii and materials. This implies that in order to slide two particles over each other, a force has to be applied that is also capable of breaking a contact. Especially in the collisions of a single grain with another grain of equal size or an aggregate of equal sized grains sliding will be a negligible process.

However, the situation is different when we consider the compaction of an aggregate in a collision with a grain that is bigger than the constituents of the aggregate. The inertia of a bigger grain is much larger and may well be sufficient to change the position of contacts in the aggrgate by sliding. The same arguments hold also in a collision between two aggregates.

As we have shown in an earlier paper (Dominik and Tielens 1995), rolling as a mechanism for moving contacts in an aggregate is possible at smaller forces that sliding. Realistic calculations of aggregate formation and in particular aggregate rearrangements in collisions should include these effects.

Acknowledgment One of the authors (CD) was supported during this work by the National Research Council. Theoretical studies of interstellar dust at NASA Ames is supported under task 399-20-01-30 through NASA's Theory Program.

References

Anderson, H. L., editor, 1981. *Physics Vademecum*. AIP, New York.

Brocklehurst, J. E., 1977. *Phys. Chem. Carbon*, **13**, 145.

Brownlee, D. E., Pilachowski, L., Olszewski, E., Hodge, P., 1979. In Halliday, I., McIntosh, B. A., editors, *Solid particles in the solar system*, IAU Symposium No. 90, Reidel, Boston.

Chokshi, A., Tielens, A. G. G. M., Hollenbach, D., 1993. *Astrophys. J.*, **407**, 806.

Derjaguin, B. V., 1934. *Koll. Z.*, **69**, 155.

Derjaguin, B. V., Muller, V. M., Toporov, Y. P., 1975. *J. Coll. Interf. Sci.*, **53**, 413.

Dominik, C., Tielens, A. G. G. M., 1995. *Phil. Mag. A*, . in press.

Easterling, K. E., Thölen, A. R., 1972. *Acta Met.*, **20**, 1001.

Frenkel, Y. I., Kontorowa, T., 1938. *Zh. Eksp. Teor. Fiz*, **8**, 1340.

Israelachvili, J., 1992. *Intermolecular and Surface Forces*. Academic Press, London, San Diego.

Johnson, K. L., 1989. *Contact Mechanics*. Cambridge University Press, Cambridge, New York.

Johnson, K. L., Kendall, K., Roberts, A. D., 1971. *Proc. R. Soc. Lond.*, **324**, 301.

Kantor, Y., Witten, T. A., 1984. *J. Physique Lett.*, **45**, L675.

Kendall, K., Alford, N. M., Birchall, J. D., 1987. *Nature*, **325**, 794.

Kinoshita, K., 1988. *Carbon*. Wiley, New York.

Kittel, C., 1976. *Introduction to Solid State Physics*. Wiley, New York.

Landman, U., Luedtke, W. D., Burnham, N. A., Colton, R. J., 1990. *Science*, **248**, 454.

Landmann, U., Luedtke, W. D., 1993. In Wiesendanger, R., Güntherodt, H.-J., editors, *Scanning Tunneling Microscopy III*, chapter 9, page 207. Springer, Berlin, Heidelberg, New York.

McClelland, G. M., 1989. In Grunze, M., Kreuzer, H. J., editors, *Adhesion and Friction*, page 1, Springer, Berlin, Heidelberg.

McClelland, G. M., Glosli, J. N., 1992. In Singer, I. L., Pollock, H. M., editors, *Fundamentals of Friction: Macroscopic and Microscopic Processes*, page 405, Kluwer, Dordrecht, Boston, London.

Reiss, H., 1968. *J. Appl. Phys.*, **29**, 5045.

Sperling, G., 1964. PhD thesis, Technische Hochschule Karlsruhe, Karlsruhe.

Tabor, D., 1992. In Singer, I. L., Pollock, H. M., editors, *Fundamentals of Friction: Macroscopic and Microscopic Processes*, page 3, Kluwer, Dordrecht, Boston, London.

Tománek, D., 1993. In Wiesendanger, R., Güntherodt, H.-J., editors, *Scanning Tunneling Microscopy III*, chapter 11, page 269. Springer, Berlin, Heidelberg, New York.

Tomlinson, G. A., 1929. *Phil. Mag.*, **7**, 905.

Zisman, W. A., 1963. *Ind. Eng. Chem.*, **55**, 19.

Material properties

Material	γ^a (mJ m^{-2})	E (N m^{-2})	ν	σ Å	b Å	Reference
Quartz	25[b]	5.4(10)	0.17	3.44	1.84	1,2,7
Graphite	75	1.0(10)	0.32	3.40	1.54	4,5,7
Iron	3000	2.1(11)	0.27	2.24	2.24	2,6,7
Ice	370[d]	7.0(9)	0.25	3.36	3.36	2,7

[a] Surface energy per surface

[b] Measured for micron-sized particles

[c] Estimated from H-bonding

References: (1) Kendall, Alford and Birchall 1987; (2) Physics Vademecum (Anderson 1981); (4) Brocklehurst 1977; (5) Zisman 1963; (6) Easterling and Thölen 1972; (7) Israelachvili 1992.

Table 1

Figure Captions

Figure 1: The different degrees of freedom of the contact between two spheres.

Figure 2: Sketch of the independent oscillator model. The sliding atom is pressed on a rigid substrate with a constant force f_z. The arising tangential force is balanced by a horizontal spring.

Figure 3: The properties of the potential V_{AB} as a function of the location x of the sliding atom. The following quantities are plotted: Top: Potential V_{AB} (full line), Force applied in x-direction f_x (broken line). Bottom: Second derivative of the potential.

Figure 4: Motion of the atom during sliding. The motion has been plotted for three different normal forces applied, which are noted above the diagrams. A value of 8(???) for the horizontal spring constant has been used. The abscissa x_0 is the equilibrium position of the sliding atom without its interaction with the substrate A (see Eq. (5)). The plotted quantities are the position x of the sliding atom on the substrate, the difference $x - x_0$ and the force f_x which is associated with this spring. The dotted line denote the equilibrium position x (first row of diagrams), zero (second row), and the mean value of the force f_x which by definition is the friction force.

Figure 5: Dependence of the maximum force in x direction $f_x^{\max}$, the critical spring constant c_{crit}, and the friction force f_x^{fric} on the applied force f_z for the model with $\sigma = b$ and with a constant normal force applied. The different curves in the uppermost panel are labeled by the horizontal spring constant assumed.

Figure 6: Approximation of a sphere with small cubes. The edge length of the cubes is 1/50 of the diameter of the sphere

Figure 7: Resistance to sliding on surfaces with steps in the surface grids. See text.

Figure 8: Resistance to sliding at zero applied load, as derived for the different processes discussed in the text. The lines in all plots are lines of constant force. Forces are normalized to the pull-off force P_c. **(a)** Maximum force for aligned identical grids, with all atoms in phase. **(b)** Minimum force, as derived for *independent* oscillators. **(c)** Friction force resulting from repeated flattening of steps inside the contact area. **(d)** The sum of (b) and (c), which is the friction force that acts over most of the surface.

Figure 9: Resistance to spinning at zero applied load, as derived for the different processes discussed in the text. The lines in all plots are lines of constant torque. Forces are normalized to $P_c a_0$. **(a)** Maximum torque for aligned identical grids, with all atoms in phase. **(b)** Minimum torque, as derived for *independent* oscillators. **(c)** Torque resulting from repeated flattening of steps inside the contact area. **(d)** The sum of (b) and (c), which is the torque that acts over most of the surface.

Figure 10: Experiment to show the distance of sliding in a typical collision between two spheres. One of the two spheres is fixed in an inertial system (hatched area). The other sphere is approaching with a kinetic energy W_0. Upon contact, the moving spheres slides over over the fixed sphere until all energy is dissipated.

Figure 11: Sliding distance of a sphere colliding with an energy $P_c\delta_0$ with an equal-size sphere. The sliding distance is normalized by the circumference of the sphere.

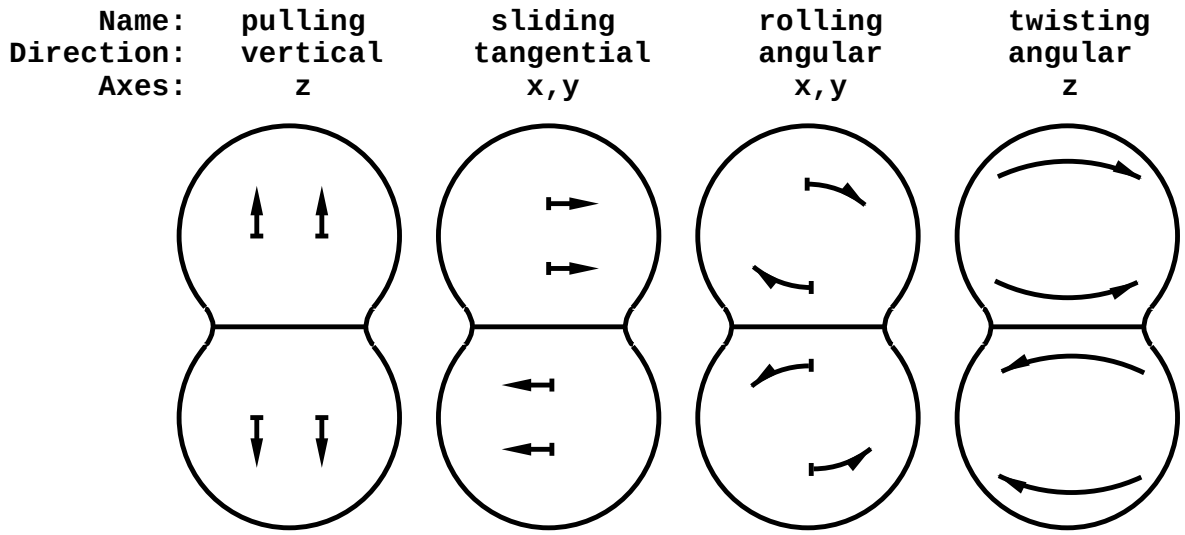
Name: pulling sliding rolling twisting
Direction: vertical tangential angular angular
Axes: z x,y x,y z

Figure 1

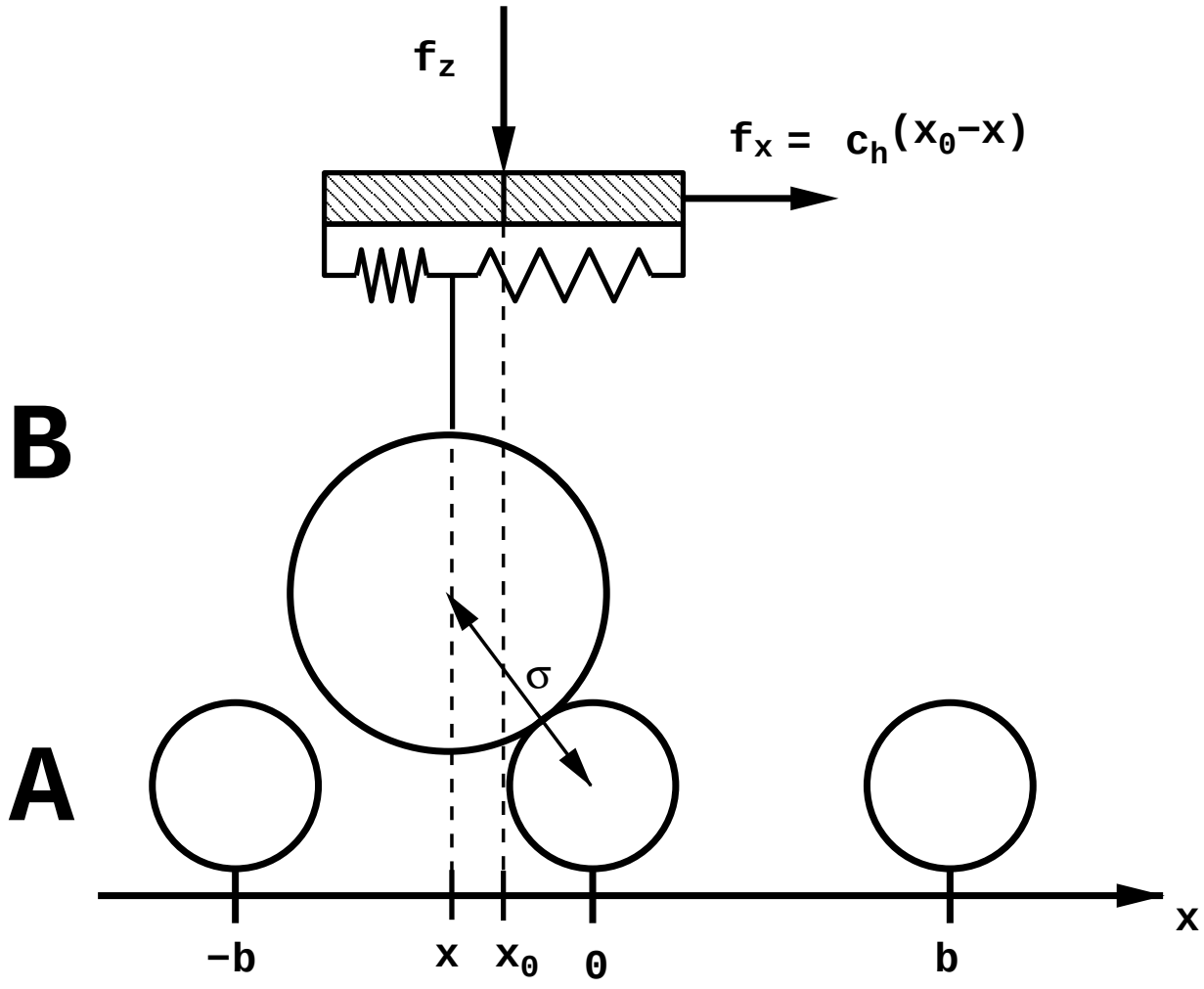

Figure 2

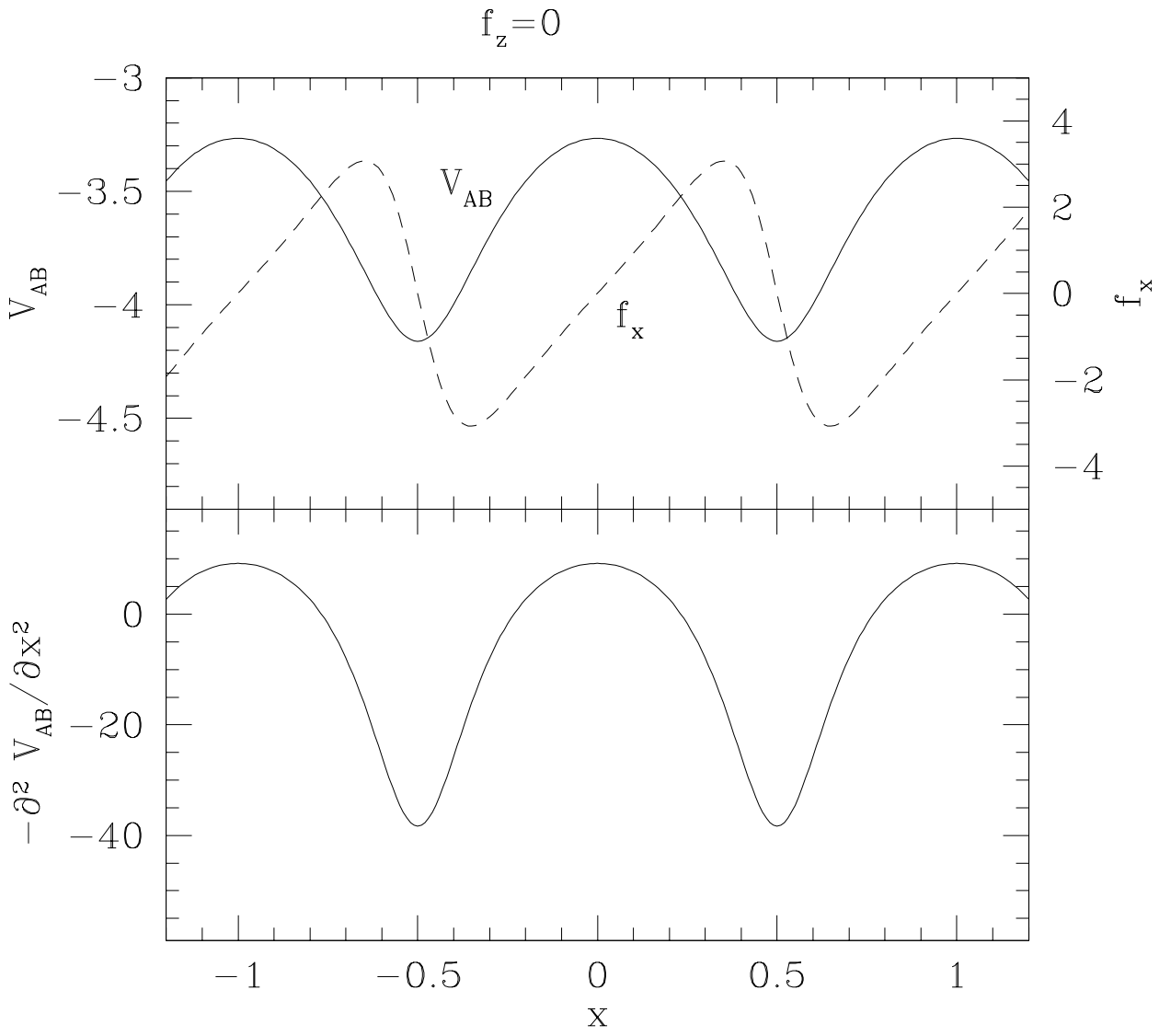

Figure 3

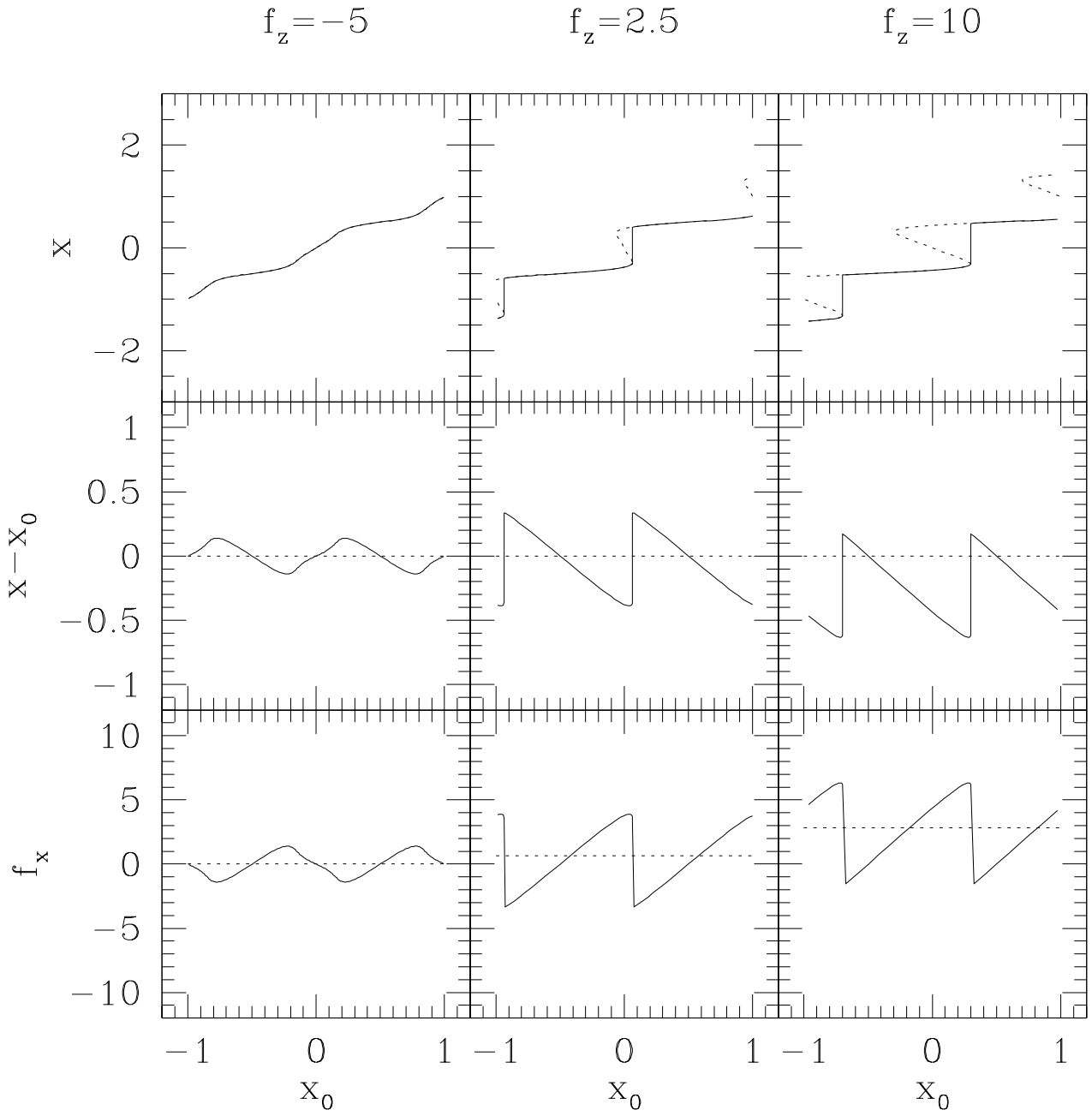

Figure 4

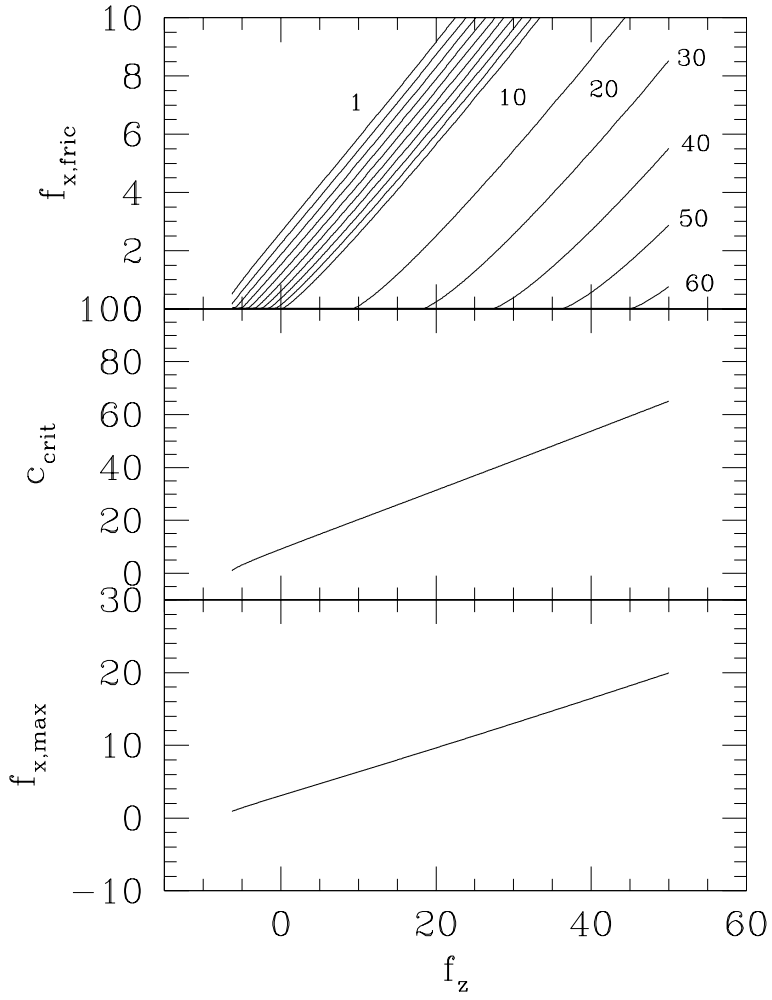
10
8
6
4
2
100
80
60
40
20
0
30
20
10
0
−10
0
20
40
60
$f_{x,fric}$
c_{crit}
$f_{x,max}$
f_z
1
10
20
30
40
50
60

Figure 5

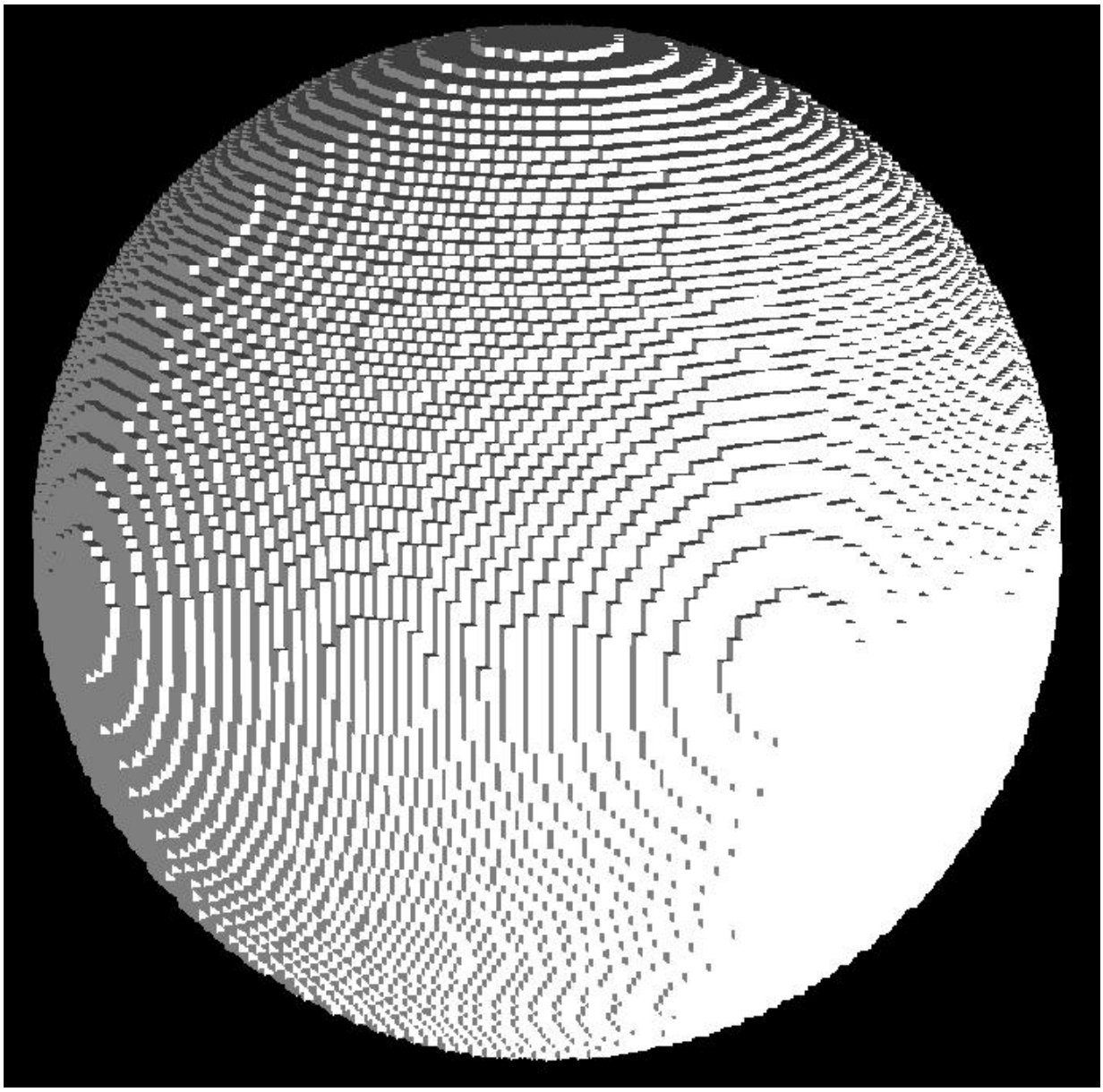

Figure 6

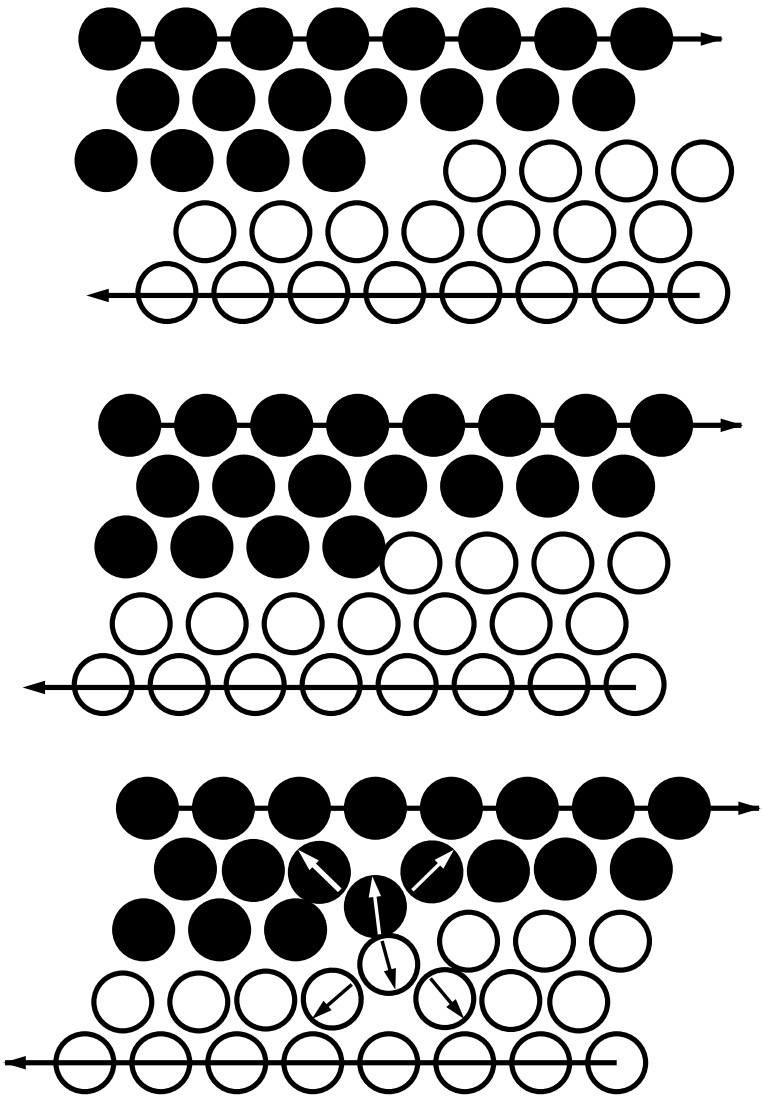

Figure 7

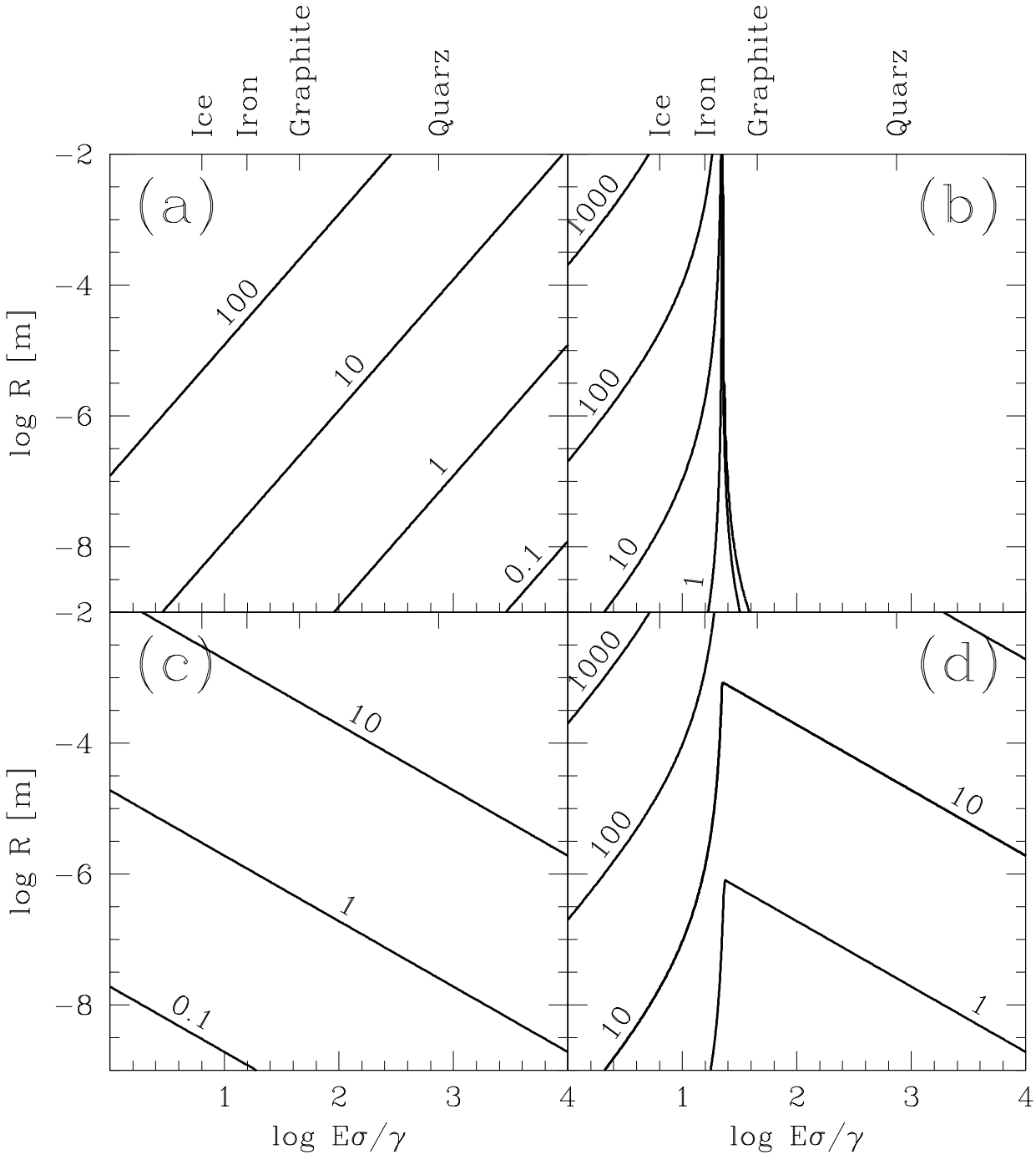
Ice
Iron
Graphite
Quarz
(a)
(b)
(c)
(d)
100
10
1
0.1
1000
log R [m]
log Eσ/γ
−2
−4
−6
−8
1
2
3
4

Figure 8

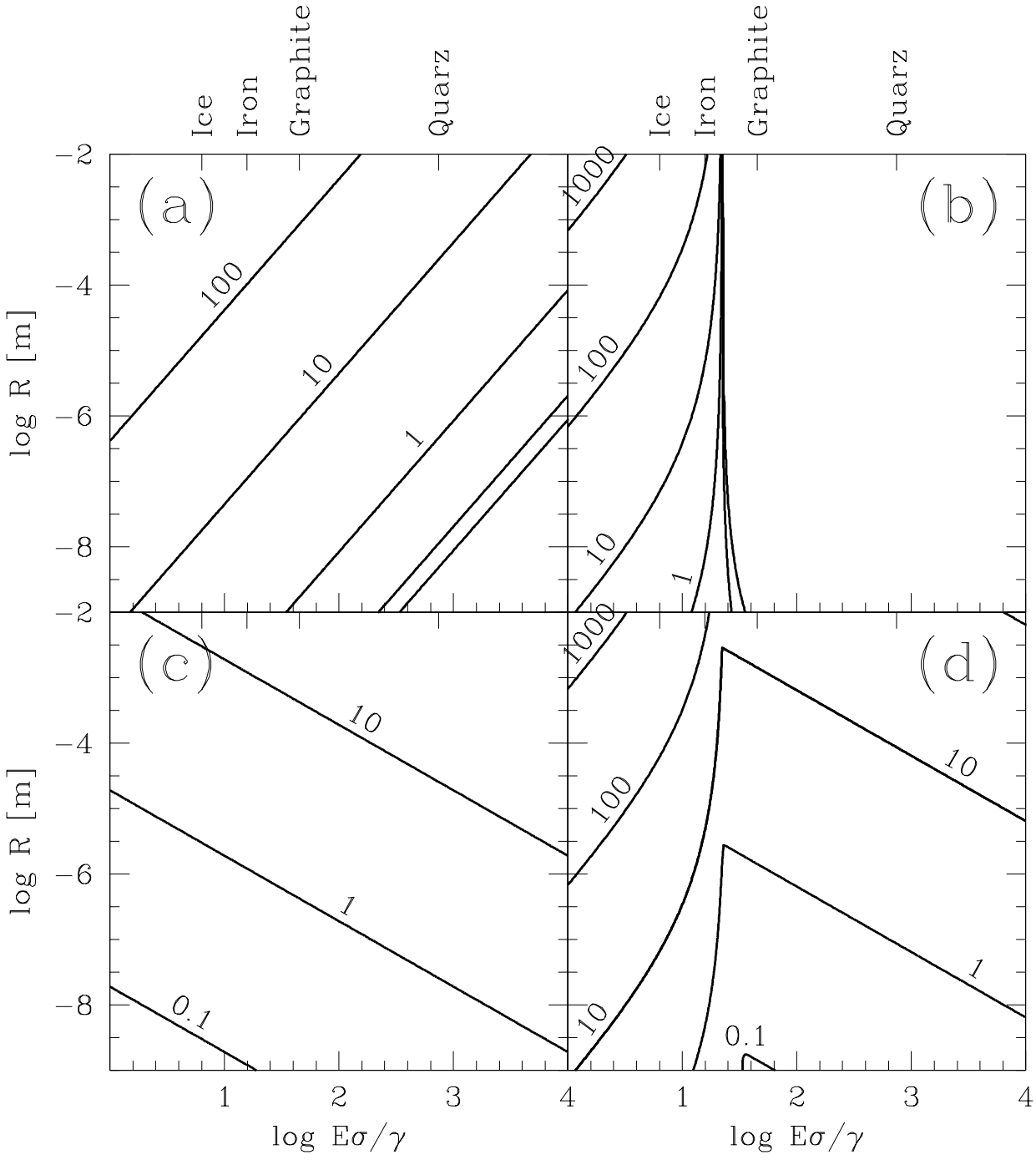
Ice
Iron
Graphite
Quarz
(a)
(b)
(c)
(d)
100
10
1
1000
0.1
log R [m]
log Eσ/γ
−2
−4
−6
−8
1
2
3
4

Figure 9

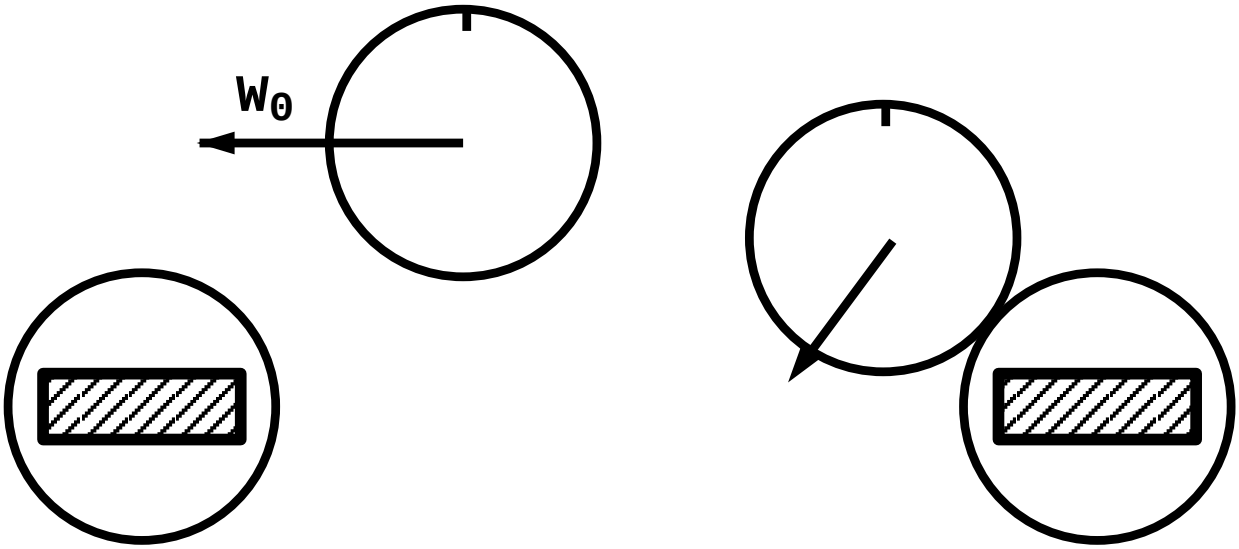

Figure 10

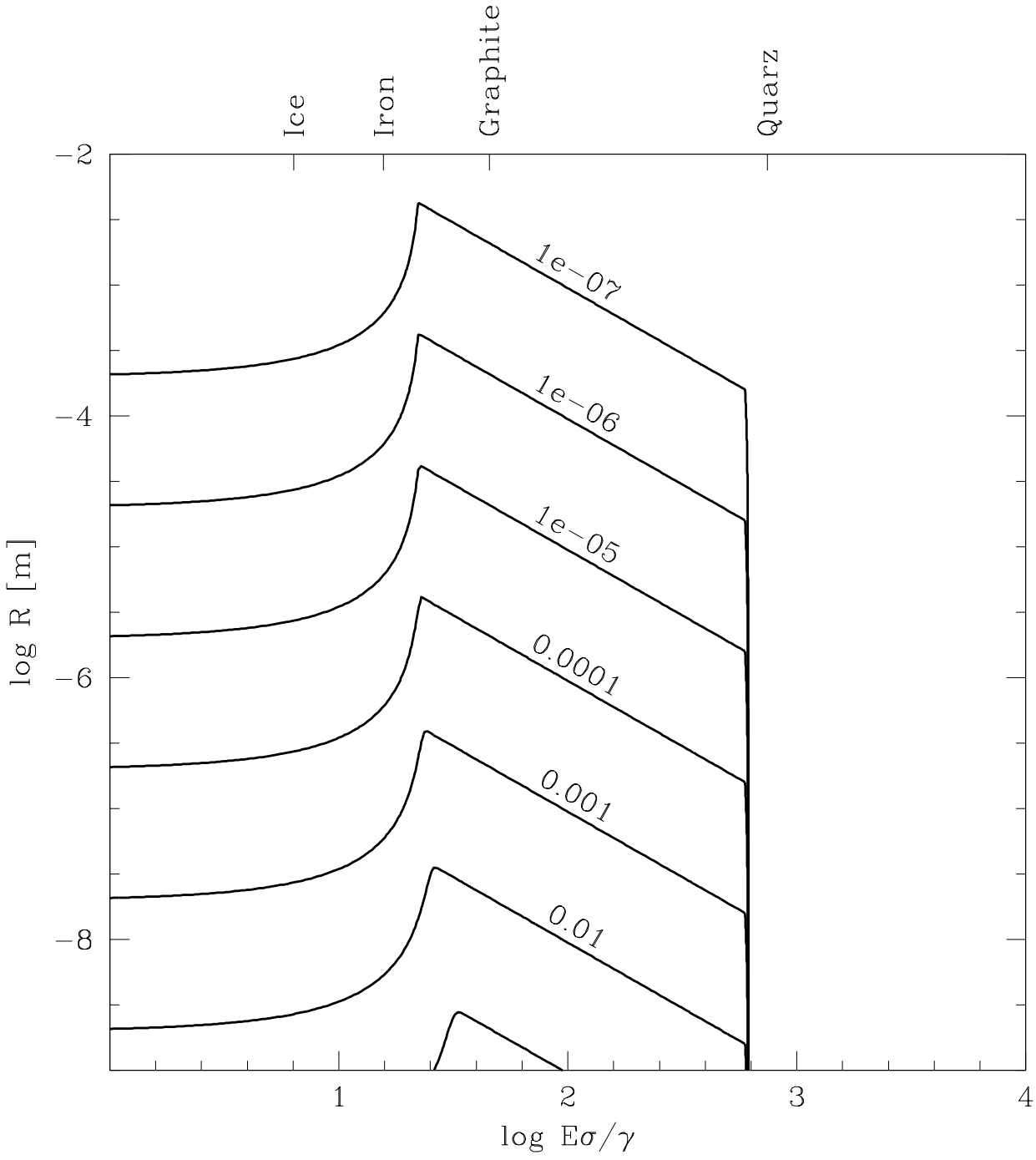
Ice
Iron
Graphite
Quarz
−2
−4
−6
−8
log R [m]
1e−07
1e−06
1e−05
0.0001
0.001
0.01
1
2
3
4
log Eσ/γ

Figure 11